Development of Thin-Window Silicon Drift Detector for X-ray spectroscopy

W. Chen , G. A. Carini, G. De Geronimo, J. Fried, J. A. Gaskin , J. W. Keister, Z. Li, B. D. Ramsey, P. Rehak and D. P. Siddons

***Abstract*– A new set of Thin-Window Silicon Drift Detectors composed of an array of hexagonal shaped detectors has been designed, constructed and tested for X-ray spectroscopy. Each individual ThinWinSDD has a thin entrance window on one side and a spiral shaped hexagonal cathode around a center anode on the other side. To produce the thin entrance window a 10 keV implantation of boron through a 500 Å silicon dioxide was used. The implantation was followed by an annealing at 700 °C for 30 min and a reactive ion etching step to ensure the removal of silicon dioxide from the smallest feature (5 µm). An aluminum layer is coated in the same vacuum system after back-sputtering. This step involves removing the native oxide that has formed on the top of the silicon substrate and then sputtering a 1100 Å thick layer of aluminum onto the X-ray entrance window. The aluminum layer must be thick enough to block visible light, but thin enough to be transparent to soft x-rays down to 280 eV. We discuss first test results that include detector leakage current measurements and the response for multiple detectors exposed to the National Synchrotron Light Source's UV beam line U3C located at Brookhaven National Laboratory for X-ray energies as low as 280 eV.**

I. Introduction

THIS work is a collaboration between the NASA Marshall Space Flight Center (MSFC) and Brookhaven National Laboratory (BNL). The detectors developed here are prototypes, indicative of the detectors to be used on future lunar missions. The purpose of such a mission would be to perform elemental mapping of the lunar surface using X-ray fluorescence. The fluorescence of the lunar surface is due to the solar X-rays.

The spectroscopic system consists of an array of collimators defining a sensitive area sweeping the lunar surface. The X-ray collimators are followed by an array of silicon drift detectors (SDDs) [1] readout with low noise electronics. They provide 1) the energy of individual X-rays for the identification of the elements and 2) the time information of the X-ray detection to assign the location of the emitting source on the lunar surface from the known trajectory of the satellite. The lightest element of interest is carbon; its K_α energy is 282 eV. This presents two main challenges for this development. First, the equivalent noise charge (ENC) of the readout electronics of each SDD should be very low, close to 10 electrons to adequately resolve the carbon K_α line. Second, the entrance window for X-ray detection should be transparent to X-rays and opaque to ambient visible light. Detailed studies showed that a 1100 Å thick layer of aluminum can sufficiently attenuate the visible light such that its impact on the SDD leakage current is negligible. These requirements drove the development of a thin-window silicon drift detector (ThinWinSDD), described below.

Manuscript received Nov 16, 2007. This work was supported in part by the U.S. Department of Energy under Contract No. DE-AC02-98CH10886.

W. Chen, G. A. Carini, G. De Geronimo, J. Fried, Z. Li, P. Rehak, and D. P. Siddons are with Brookhaven National Laboratory, Upton, NY 11973, USA

J. A. Gaskin and B. Ramsey are with MSFC/National Space Science and Technology Center, Huntsville, AL 35805, USA

J. W. Keister is with SFA Inc., Brookhaven National Laboratory, Upton, New York 11973

II. Detector Design and Function

The ThinWinSDD has been designed in such a way that it has a thin junction that covers the entire active area on the window side. The complete assembly consists of an array of 14 pixels on the device side with an additional two test pixels at two of the corners. There are 4 guard rings surrounding the 14-pixel array area on both sides of the detector. Each pixel is a hexagonal spiral drift detector. Within an array, 7 of the pixels have an aluminum field plate which intended to stabilize the field distribution under the Si-SiO_2 and the other 7 do not. Figure 1 shows a three and two dimensional drawing of the device. There is a thin junction on the window side which is covered with a thin aluminum contact. On the device side a hexagonal shaped cathode surrounds a central anode. Immediately around this central anode is a hexagonal shaped rectifying contact, E1. Another contact in the outer portion of the spiral is common to all 14 pixels. The desired voltage supplied to these two contacts creates a current which flows from the inner end of the rectifying spiral to the outer end of the spiral and at the same time generates a potential gradient inside the hexagon volume. To minimize power usage it is not practical to keep the temperature of the detector array below -30 ºC. In order to satisfy this requirement we designed an additional feature called the sink anode. It is designed in such a way that the surface current, which is generated from the Si-SiO_2 interface under the oxide spiral, is directed towards the sink anode and removed through the E1 contact. This is done via a small bridge connection between the E1 and the sink anode. The values of the pitch and of the width of the spiral were calculated so as to provide an optimal drift electric field within the volume of the hexagon [2,3].

When the X-rays enter the detector's volume, they generate electron-hole pairs. The electrons drift along the potential gradient toward the center anode and then are read out by the electronics. The holes move to the rectifying spiral surface flowing toward the outer end of the spiral. The area of a single

pixel is 16 mm^2 where the dimension "a" is 2.48 mm and the dimension "h" is 2.15 mm (Fig. 1c). The area of center anode is 0.01 mm^2.

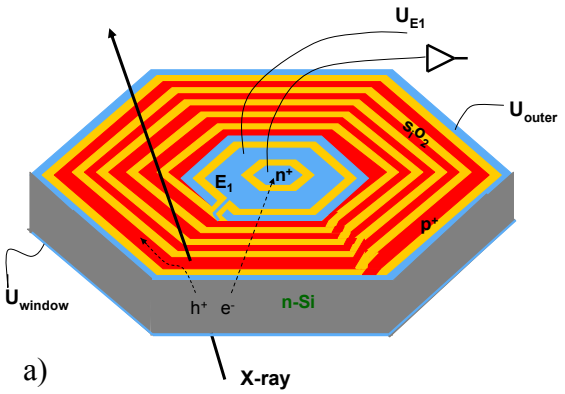

a)

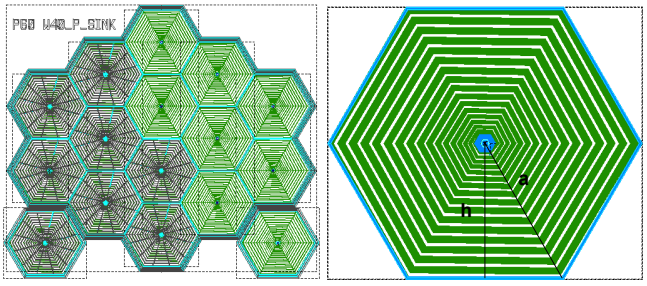

b) c)

Fig. 1. Three and two dimensional figures of a single pixel and two dimensional array of the ThinWinSDDs.

III. Fabrication of the Detectors

To date, we have fabricated several ThinWinSDD arrays each with different parameters. The SILVACO simulation results and the X-ray responsivity measurements of the test devices at the National Synchrotron Light Source (NSLS) (Fig. 2) showed that the 10 keV boron implanted through a 500 Å silicon dioxide yields the thinnest possible dead layer and junction [4].

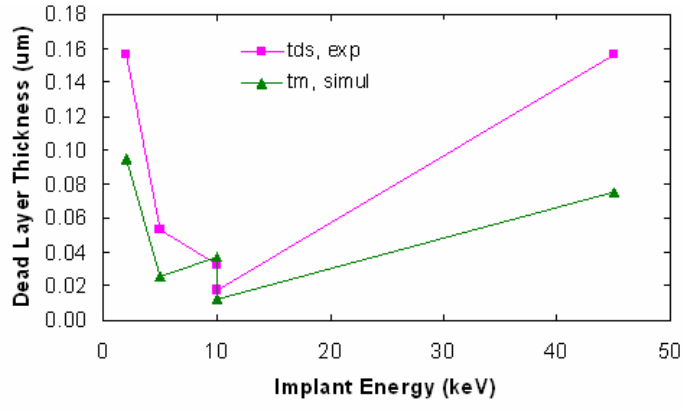

Impl (keV)	Dose (cm^{-2})	Annealing	Back Sputter	t_{Si} (dead) (Å)	Al (Å)
45 (1000 SiO_2)	$1x10^{15}$	700 °C, 17 h	N	1560	1800
10 (500 SiO_2)	$1x10^{14}$	700 °C, 17 h	N	182	1800
2	$1x10^{15}$	700 °C, 17 h	N	1560	1800
5	$1x10^{14}$	700 °C, 30 min	Y	533	1800
10	$1x10^{14}$	700 °C, 30 min	Y	332	1800

Fig. 2. SILVACO simulation and DC current experimental results on the dead layer thickness versus the implantation energies. The corresponding fabrication parameters are listed in the table.

ThinWinSDD's were fabricated on n-type (111) silicon substrates with a thickness of 350 µm and a resistivity of 4 ~ 6 kΩ·cm. The partial cross section of the detector is showing in Fig. 3.

The processing on the window side is as the following: to produce the thin entrance window of ThinWinSDD, a 10 keV ($1x10^{14}$/cm^2) boron implantation through a 500 Å silicon dioxide was used. Back-sputtering was performed to remove the native silicon dioxide. An 1100 Å thick aluminum layer was coated in the same vacuum system on the window side as required. Therefore the entrance window is radiation hard due to the lack of silicon dioxide between the thin-junction and the aluminum layer.

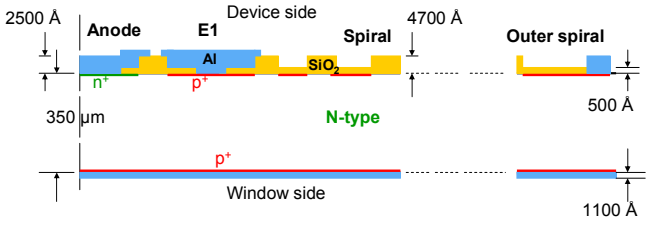

Fig. 3. A partial cross section of a pixel of the ThinWinSDD.

On the device side, the original 4700 Å of silicon dioxide has been etched down to 500 Å at the spiral. A 10 keV ($1x10^{15}$/cm^2) boron implantation through 500 Å of silicon dioxide was used to generate the p^+ spiral. Then the silicon dioxide was removed completely at the center anode and at the sink anode for a 10 keV ($1x10^{14}$/cm^2) phosphorus ion implantation while the spiral region is covered by aluminum mask. The implantation was followed by an annealing at 700 °C for 30 min. Reactive Ion Etching (RIE) was then performed to remove the 500 Å silicon dioxide layer which covered the metal contact locations. RIE also ensures the removal of residual silicon dioxide from even the smallest features (5 µm). A layer of 2500 Å aluminum was deposited following the back-sputtering. Back-sputtering is used to remove the native silicon dioxide prior to the deposition of the aluminum. The entire fabrication of the ThinWinSDD array involves 7 masks and consists of 8 mask steps. Each finished wafer contains 12 arrays that were cut into individual devices for

testing. The detectors with and without the aluminum field plate design are shown in Fig. 4 c and 4 d respectively.

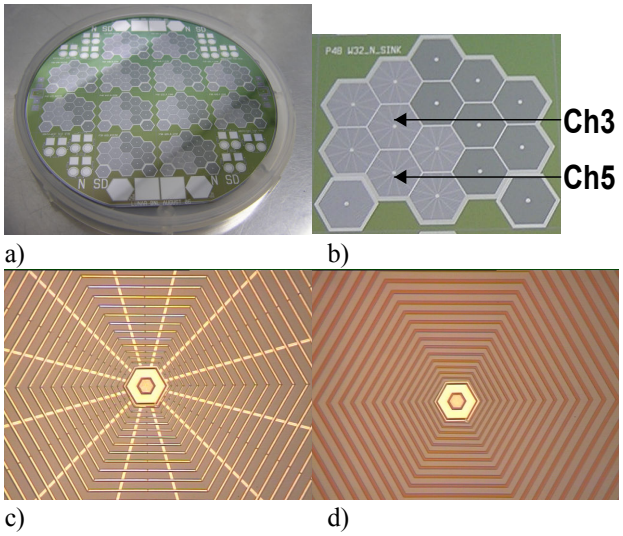

Fig. 4. a) Image of a finished wafer with several ThinWinSDD arrays. b) Image of a single array. c) SDD with an aluminum field plate design. d) SDD without an aluminum field plate.

IV. Test Results and Discussions

The results from two selected arrays, labeled B1531 and K19, are reported here. B stands for the detectors fabricated in BNL while K stands for the ones from KETEK. These arrays were biased according to the following configuration: U_{window} was set at -100 V for B1531 and at -80 V for K19[1]. The bias at E1, U_{E1}, was set to -20 V. The leakage current was measured from the center anode at room temperature while U_{outer} was systematically varied from -10 V to -120 V as shown in Fig. 1a considering without incident X-ray. The B1531 and K19 behave very similarly. All 14 pixels' leakage currents were plotted for each array (Fig. 5). The most of the pixels have leakage current below few nA when U_{outer} is -100 V at room temperature. However a few of the pixels are still measured higher than few nA leakage current. The effort for producing more uniform pixels is needed. We notice that there are both good and worst or "noisier" pixels for both field-plate and no-field-plate designs in this leakage current test.

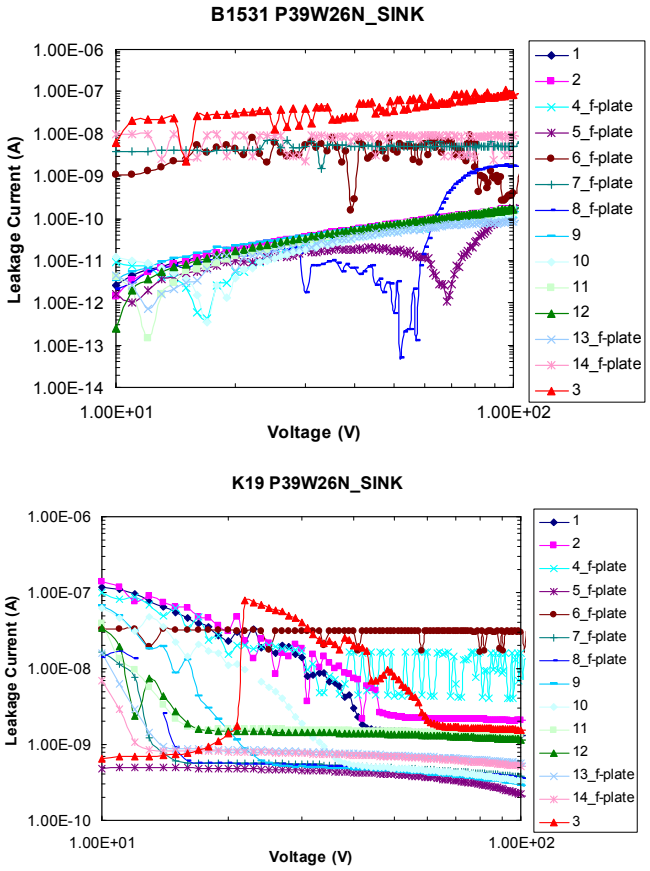

Fig. 5. Leakage current was measured for all 14 pixels in an array from the center anode at room temperature for both detectors. U_{outer} was varied from -10 V to -120 V.

The K19 array was then wire-bounded to a specially designed low noise ASIC and read out with a PCI (peripheral component interconnect) based and LabView (graphic software interface) controlled custom data acquisition (DAQ) system [5]. The entire array was successfully tested in the NSLS UV beam line, U3C [6] at the BNL. This beam line is used for absolute radiometric calibration in the 50 to 1000 eV X-ray range [7, 8]. The detector was biased in such a way that U_{window} was -132 V, U_{E1} was -7.4 V and U_{outer} was -178 V. The complete assemblies were cooled to -34ºC. The actual detector temperature was estimated to be around -25ºC.

Histograms of 900 eV X-rays incident on a single pixel in the K19 array were taken by using the LabView system and also by using an oscilloscope direct screen shot (Fig. 6). The main peak corresponding to 900 eV incident X-rays is obvious, However, we also noticed a smaller peak that was present in both histograms. We also performed X-ray scans at 900 eV across a single detector. Fig. 7 shows these scan results, a) for a scan in a distance of 2a (Fig. 1c), and b) for a scan in a distance of 2h across two neighboring pixels. From these results it is evident that the pixel is indeed sensitive across a distance of about 5 mm (in the 2a direction). When scanned across each pixel in the 2h dimension, each pixel is

[1] According to NASA's policy that products can not come only from one source. We also acquired same products from KETEK.

similarly sensitive, even across the boundary between two pixels. Histograms were also taken at 700 eV are shown in Fig. 8. The main peak corresponding to 700 eV is still obvious. In contrast, the smaller peak-"niose", seen in the 900 eV case, becomes more significant.

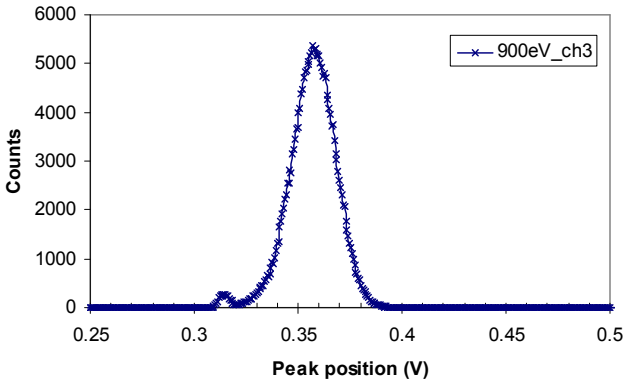

a)

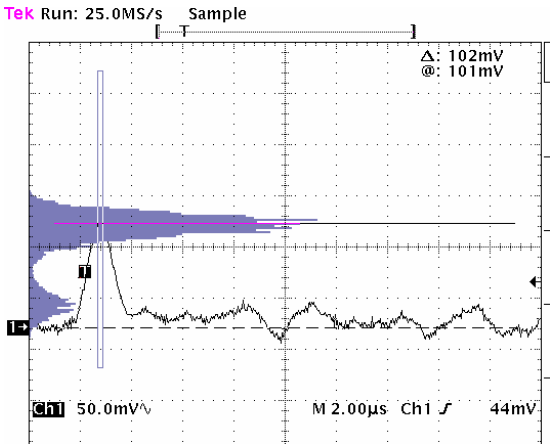

b)

Fig. 6. The histogram of 900 eV X-rays were taken a) by LabView data acquisition system and b) by direct screen shot of an oscilloscope.

In the cases of 400 eV and 280 eV X-ray's, the main peak are completely merged into this smaller peak. Fig. 9 shows the histograms collected by a LabView controlled DAQ normalized to total counts. The detected peak positions of 900 eV, 700 eV X-rays are clearly seen, while those of 400 eV and 280 eV X-ray's are barely visible. To check if the peaks we have seen corresponding to 400 eV and 280 eV are not the part of the "niose" in Fig. 9, we measured the same pixel for the beam on and off condition respectively to see the detector's response for the 400 eV and 280 eV X-rays. The screen shot results of an oscilloscope are shown in Fig. 10, we can clearly see that the peak position shifts, corresponding to when the beam is turned on and off for both 400 eV and 280 eV. Therefore the detector can sense the 400 eV and 280 eV X-ray.

The reason for these not as good spectroscopy results for the 400 eV and 280 eV X-ray can be various. One thing is sure that the detector system was not operated at the optimum condition due to the short time for test beam period at NSLS: the detector may not be biased at the optimum combination of voltages; the shielding of the system was not good enough from the possible noise sources such as the computer, the power line; etc. Further work and investigations, including the optimization of the detector design, fabrication, ASIC, interconnect, and custom DAQ designs are certainly required to achieve much better spectroscopy results for the 280 eV X-ray.

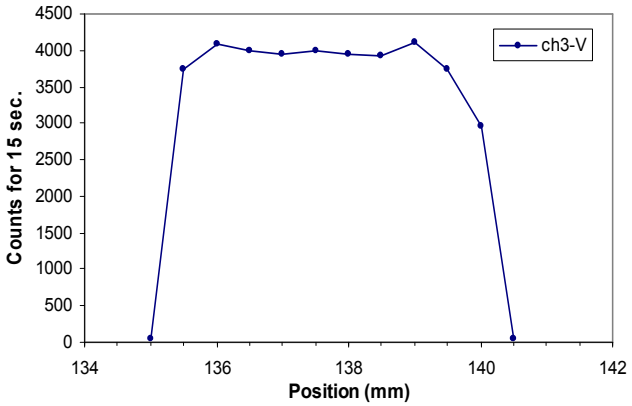

a)

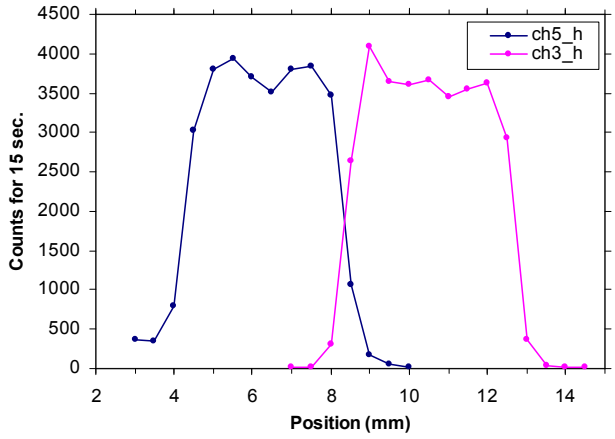

b)

Fig. 7. The scan results of 900 eV X-ray across a) 2a distance of a pixel, and b) 2h distance for each pixel of two pixel scan.

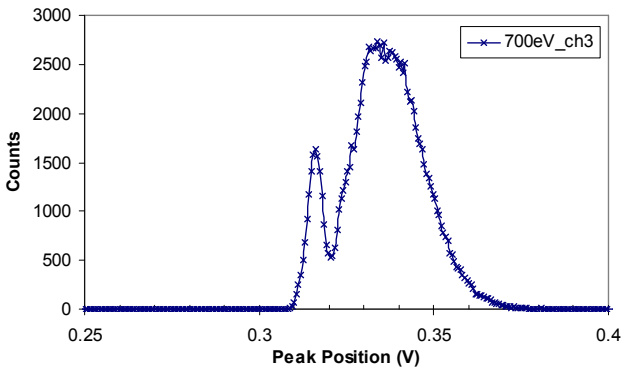

a)

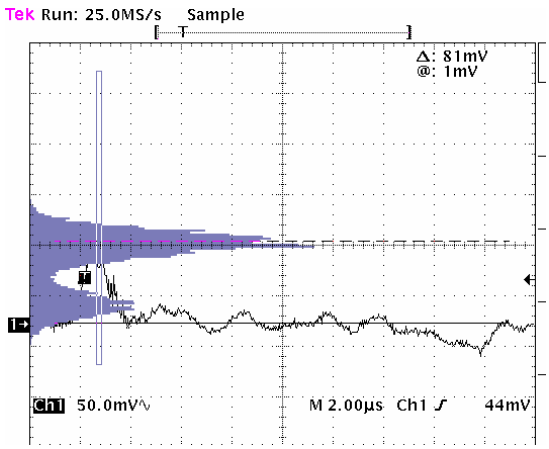

b)

Fig. 8. The histogram of 700 eV X-rays were taken a) by LabView data acquisition system and b) by direct screen shot of an oscilloscope.

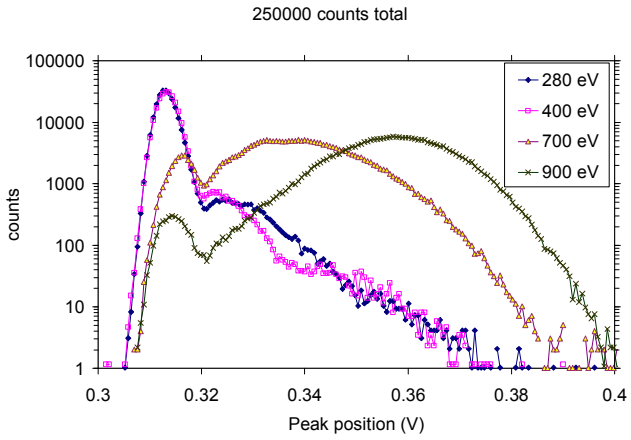

Fig. 9. The histogram of peak positions corresponding to 900 eV, 700 eV, 400 eV and 280 eV X-rays normalized to the total counts.

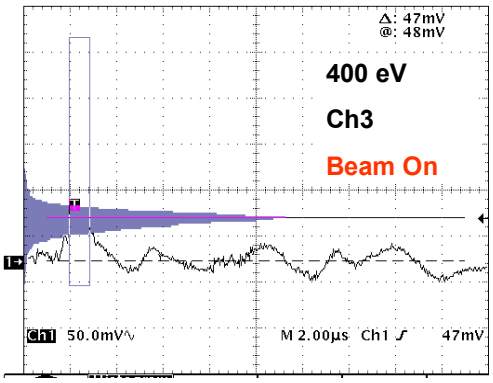

a)

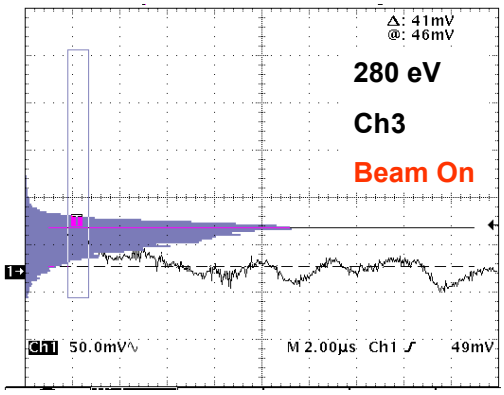

b)

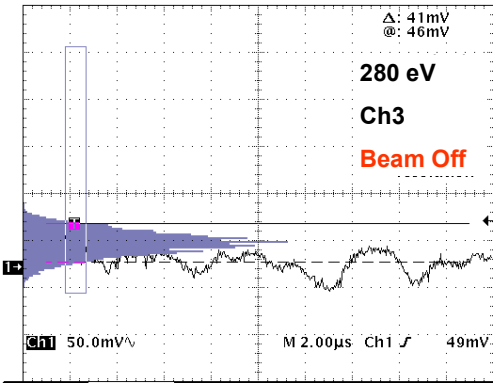

c)

Fig. 10. Histograms were taken by an oscilloscope a) for 400 eV when the beam is turned on, b) for 280 eV when the beam is turned on, c) when the beam is turned off.

V. Conclusion

The prototype ThinWinSDD array has been designed, fabricated and tested. X-rays of 900 eV and 700 eV have been detected spectroscopically. X-rays of 400 eV and 280 eV have been sensed by the detector. The limitation on spectroscopic detection for 400 eV and 280 eV was due to a source, still under investigation. Future work includes optimization of the detector design, improved fabrication, modified ASIC, improved interconnect scheme and DAQ designs in order to achieve the spectroscopic measurement of the 280 eV line.

ACKNOWLEDGMENTS

We would like to express our sincere appreciation for the continued support of R. Beuttenmuller and D. Elliott given to us over the years. We also like to express our thanks to J. Fried, D. Pinelli, J. Triolo, E. Vernon, T. Lenhard for their assistance on the data acquisition system, bonding of the array to the PC board, making connection of the wires, identifying the channel of ASIC and the design of the cooling system. We are thankful to KETEK for supplying some of the detectors.

REFERENCES

[1] E. Gatti and P. Rehak, "Semiconductor Drift Chamber—An Application of a Novel Charge Transport Scheme," Nucl. Instr. And Meth., vol. 225, p608, 1984.

[2] P. Rehak, E. Gatti, A. Longoni, M. Sampietro, P. Holl, G. Lutz, J. Kemmer, U. Prechtel, and T. Ziemann, "Spiral Silicon Drift Detectors", IEEE transaction on Nucl. Science, vol. 36, No 1, 203-209, Feb. 1989.

[3] W. Chen, E. Gatti, and P. Rehak, "P-type one-sided hexagonal spiral drift detectors", IEEE Trans. Nucl. Sci. vol. 51.989-994, 2004

[4] W. Chen, G. Carini, J. Keister, Z. Li and P. Rehak, "Development of Thin-junction Detector", To be published in IEEE Trans. Nuc. Sci. in Aug. 2007.

[5] Gianluigi De Geroimo, Wei Chen, Jack Fried, Zheng Li, Donald A. Pinelli, Pavel Rehak, Emerson Vernon, Jessica A. Gaskin, Brian D. Ramsey, and Giovanni Anelli, "Front-end ASIC for High Resolution X-Ray Spectrometers", Proc. 2007 IEEE Nucl. Sci. Symp., Hawaii, Oct. 2007

[6] http://www.bnl.gov/u3cx8a and/or http://www.nsls.bnl.gov/beamlines/beamline.asp?blid=U3C

[7] R. J. Bartlett, W. J. Trela, F. D. Michaud, et al "Characteristics and performance of the Los Alamos VUV beam line at the NSLS", Nucl. Istr. Meth. A266 (1988) 199.

[8] J. W. Keister "Silicon photodiodes for absolute soft x-ray radiometry", Proc. SPIE Vol. 6689 66890U (2007)